

# Microstructural Effect on Creep of SiAlON Ceramics

Alper Uludag

Faculty of Aeronautics and Astronautics

Anadolu University

Eskisehir, Turkey

alperuludag@anadolu.edu.tr

**Abstract**—SiAlON ceramics have received increasing attention in recent years, because of their excellent properties such as high flexural strength, high fracture resistance, good creep resistance, high hardness and excellent wear resistance. These excellent properties depends on the development of microstructures.

Creep is the time-dependent and permanent plastic deformation of a material subjected to stress at high temperatures. The creep behavior of materials can be determined by a combination of creep testing and microstructural evaluation.

In this study microstructural effect on creep of SiAlON ceramics were investigated.

**Keywords**— SiAlON Ceramics; Microstructure; Creep; Four point bending

## I. INTRODUCTION

Silicon nitride ( $\text{Si}_3\text{N}_4$ ) is one of the major structural ceramics that has been developed following many years of intensive research. It possesses high flexural strength, high fracture resistance, good creep resistance, high hardness and excellent wear resistance [1]. These excellent properties offer a potential for use in structural applications [2]. Silicon nitride turbocharger rotor is shown by Fig. 1.

These excellent properties depends on the development of microstructures through the processing of the ceramic [3]. The properties of silicon nitride materials can vary with their microstructures depending on the starting materials and on the method used for sintering as well as the post heat treatment [2-4].



Fig. 1. Silicon nitride turbocharger rotor [3]

Because of the highly covalent bonding with a low self-diffusion coefficient of  $\text{Si}_3\text{N}_4$ , the addition of some oxides or nitride sintering additives to the starting  $\text{Si}_3\text{N}_4$  powder is required in order to fabricate high-density  $\text{Si}_3\text{N}_4$  ceramics by different sintering routes such as liquid phase sintering [5, 6]. During sintering, additives such as yttrium or rare earth oxides (with alumina) react with surface oxides on the silicon nitride particles and some of the nitride itself and form a M-Si-(Al)-O-N liquid (M=Y or Ln) which after cooling remains as a glass at triple junctions and grain boundaries [7]. Liquid phase sintering results in full densification and formation of microstructure consisting of high aspect ratio  $\beta$ - $\text{Si}_3\text{N}_4$  grains surrounded by a grain boundary amorphous grain boundary phase leading to excellent fracture toughness and high strength. Fig. 2 shows scanning electron micrograph of silicon nitride densified with  $\text{Y}_2\text{O}_3 + \text{Al}_2\text{O}_3$  and shows the elongated rod-like  $\beta$ - $\text{Si}_3\text{N}_4$  grains surrounded by a Y-Si-Al-O-N glass phase [3].

The presence of these amorphous grain boundary phases results in lower mechanical properties such as creep and oxidation resistance at temperatures exceeding the softening point of the amorphous phase (about  $1000^\circ\text{C}$ ) [8]. Therefore, the intergranular phases are critically important in determining the mechanical and chemical properties of  $\text{Si}_3\text{N}_4$  based ceramics particularly at high temperatures. It has been observed that the onset of creep deformation and degradation of strength in such materials can be significantly reduced by decreasing the amount of intergranular amorphous phase or by modifying it to produce more refractory crystalline phases [9 -11].

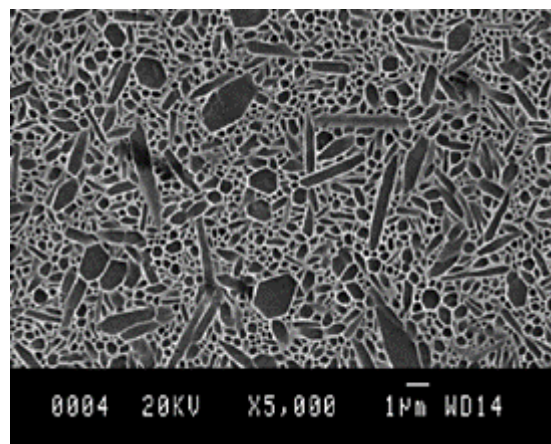


Fig. 2. Scanning electron micrograph of  $\text{Si}_3\text{N}_4$  [3]

One way of decreasing the amount of intergranular amorphous phase or by modifying it to produce more refractory crystalline phases is producing SiAlON ceramics [12]. SiAlON ceramics are  $\text{Si}_3\text{N}_4$  solid solutions containing alumina ( $\text{Al}_2\text{O}_3$ ) along with other metal oxides. SiAlONs generally consist of two crystalline phases:  $\alpha$ -SiAlON and  $\beta$ -SiAlON which are isostructural with  $\alpha$ - $\text{Si}_3\text{N}_4$  and  $\beta$ - $\text{Si}_3\text{N}_4$ , respectively [14]. An important advantage of  $\alpha$ -SiAlONs is that the amount of intergranular phase is reduced by the transient liquid phase being absorbed into the matrix of  $\alpha$ -SiAlON phase during sintering. As  $\alpha$ -SiAlON and  $\beta$ -SiAlON phases are completely compatible, SiAlON ceramics with both higher hardness and higher toughness can be achieved through designing of  $\alpha/\beta$ -SiAlON composites. Therefore, in recent years  $\alpha/\beta$ -SiAlON ceramics have received increasing attention because of their easier fabrication compared with  $\text{Si}_3\text{N}_4$  ceramics and offering more freedom for tailoring to specific applications through changes in composition and heat treatments [14 - 16]. These properties makes SiAlONs particularly attractive for high-temperature applications.

High-temperature applications have various life-limiting failure types. One of them is creep. Creep is the time-dependent and permanent plastic deformation of a material subjected to stress at elevated temperatures. The creep behavior of materials can be determined by a combination of creep testing and microstructural evaluation [17]. In this study microstructure of SiAlON ceramics before and after creep tests were investigated.

## II. EXPERIMENTAL PROCEDURE

After full dense the creep test specimens were sintered, the creep test specimens were first machined by surface grinding in a direction parallel to the length of the fully densified specimens with 80–350 grit diamond resinoid bonded wheels until having dimensions of 3 mm in height, 4 mm in width, and 50 mm in length. They were then mechanically polished and the edges of all specimens were chamfered before the creep tests.

The creep test is intended to evaluate the deformation of a test piece under nominally constant stress as a function of time at elevated temperatures. In particular it can be used for materials comparison, or for determining the temperature at which creep deformation becomes significant for a prospective engineering use. The four point bending creep method involves supporting a bar test piece on two supports near its ends, heating it to the required elevated temperature which is maintained constant, applying a force to two loading points spaced symmetrically between the support points, and recording the deflection of the test bar with time (Fig. 3) [18].

Creep tests were conducted on four-point bending fixture made of SiC with inner and outer span of 20 mm and 40 mm, respectively by using of an Instron 5581 testing machine (Fig. 4).

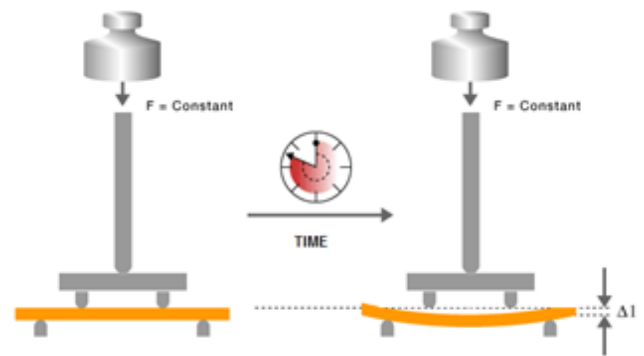


Fig. 3. Flexure creep deformation



Fig. 4. Instron 5581 testing machine

Test specimens were nominally 3 mm in height, 4 mm in width, and 50 mm in length. The fixture assembly with mounted specimen was then placed between two rigid SiC supports connected to the Alumina push rods of the creep tester. An initial preload of 20 N was applied to the specimen and maintained until the actual testing load applied.

The specimens were heated by molybdenum disilicate elements in the furnace and a Pt–Rh thermocouple was used to monitor the temperature through a programmable controller, which offered  $\pm 1^\circ\text{C}$  of temperature control. The temperature increased at a rate of about  $5^\circ\text{C}$  per minute, and the system was held at given temperature for 0.5 hour before loading. The flexure creep strain of the creep specimen was measured by using transducer rod connected to a linear-variable differential transducer (LVDT) and recorded by a computer. The creep strain of the outer fiber surface of the creep specimen was measured by transducer rod connected to a linear-variable differential transducer (LVDT) and recorded by a personal computer.

The phase compositions and substitution levels as-sintered and crept samples were determined by using an X-ray powder diffractometer (XRD, Rigaku Rint 2000).

For microstructure characterization, some parts of sintered and crept specimens were cut and mounted. The samples were polished and then coated by gold. And finally the microstructures of sintered and crept samples were investigated by using scanning electron microscope (SEM-ZEISS SUPRA 50 VP) attached with an energy dispersive X-ray spectrometer (EDX Oxford Inca) (Fig. 5).



Fig. 5. Scanning Electron Microscope

### III. RESULTS AND DISCUSSIONS

#### A. Microstructure and Phase Composition of Materials Before Creep Tests

The photo of a typical sintered  $\alpha/\beta$ -SiAlON ceramic creep test specimen is shown in Fig. 6. The upper one shows the dimensions of specimen after sintering process. After grinding process specimens have dimensions of 3 mm in height, 4 mm in width, and 50 mm in length.



Fig. 6. Photo of as-sintered  $\alpha/\beta$ -SiAlON ceramic creep test specimen before and after grinding

The back-scattered SEM images of as-sintered  $\alpha/\beta$ -SiAlON composite are given in Fig. 7 and Fig. 8 with different magnifications. Fig. 8 showing that the microstructure consists of  $\alpha$  and  $\beta$ -SiAlON grains, and triple-junction pockets filled with remains of the liquid formed during sintering. This back scattered SEM image very clearly distinguishes between the various phases;  $\beta$ -SiAlON grains, which contain no rare earth element are black colored and more needlelike, whereas  $\alpha$ -SiAlON grains, which contain small amount

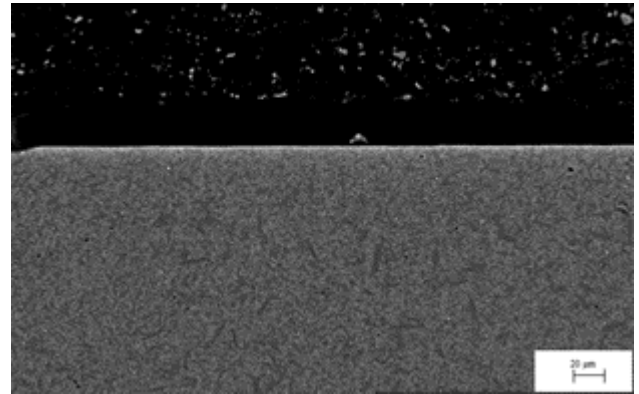


Fig. 7. Back-scattered SEM image of a cross section of the specimen (1000 x)

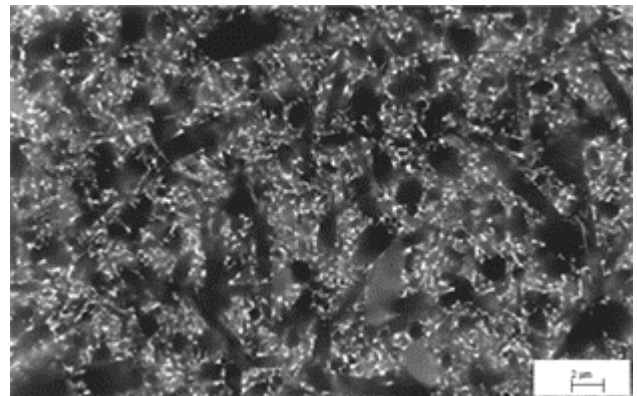


Fig. 8. Back-scattered SEM image of sintered  $\alpha/\beta$ -SiAlON ceramic (10000 x)

of rare earth element, are grey colored and more equiaxed whilst rare earth rich glassy or crystalline phases appear fine grained and white colored, because of high rare earth content. The triple-junction regions were homogeneously distributed throughout the samples.

#### B. Creep Testing

In this study four point bending creep tests were conducted in air at temperature of 1400°C and under stress levels ranging from 50 to 150 MPa to evaluate microstructures of SiAlON ceramics after creep tests. The flexure creep strain–time curves obtained in air at temperature of 1400°C and under stress levels ranging from 50 to 150 MPa is given in Fig. 9.

All tests were finished after 72 hours, without evidence of macroscopic failure. All the measured flexure creep strain-time curves show primary and secondary creep, but no tertiary creep. Si<sub>3</sub>N<sub>4</sub> based ceramics typically show only primary and secondary creep [8, 12]. The mechanisms that cause creep and the creep rates of Si<sub>3</sub>N<sub>4</sub> and SiAlONs containing intergranular amorphous phase are viscous flow, solution–precipitation, diffusion, grain boundary sliding and cavitation. Detailed the creep deformation mechanism were investigated at previous work [19].

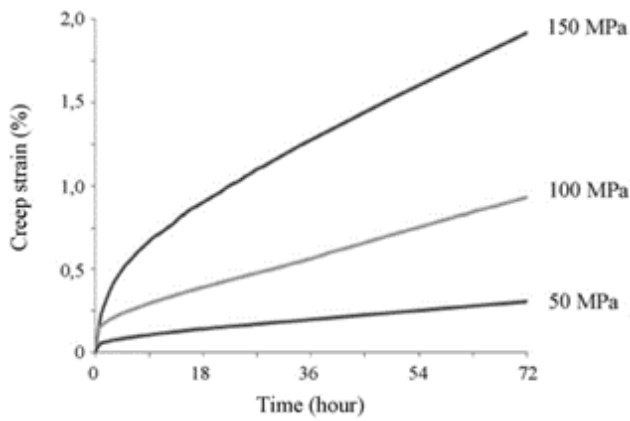


Fig. 9. Creep behavior of as-sintered  $\alpha/\beta$ -SiAlON ceramic at temperature of 1400°C as a function stress

### C. Microstructure and Phase Composition of Crept Materials

Photos of a typical sintered and crept  $\alpha/\beta$ -SiAlON ceramic creep test specimens are shown in Fig. 10. The Specimen shown below was crept more than 1.5 % strain (Fig. 10 b).

The color of the specimens changed from dark brown to almost white after creep test. This color change occurred due to oxidation. This material were exposed to high temperatures for long times in an air which is an oxidizing atmosphere. So visual observation of crept specimen surfaces reveals oxidation related effects.

The back-scattered SEM image of crept  $\alpha/\beta$ -SiAlON composite is given in Fig. 11 and Fig. 12.



Fig. 10. Photos of (a) as-sintered and (b) crept  $\alpha/\beta$ -SiAlON ceramic creep test specimens

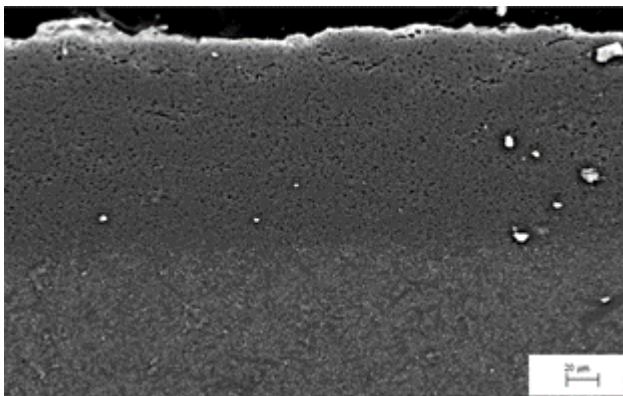


Fig. 11. Back-scattered SEM image of a cross section of the crept specimen (1300 x)

Fig. 11 demonstrates the back-scattered SEM image of across section cut from the crept sample shows the surface of oxidation scale. Several sub-layers resulted from oxidation can be visually distinguished on cross section in Fig. 11 and Fig. 12. The surface of oxide scale on crept specimen are showed Fig. 13 and Fig. 14.

XRD analysis of as-sintered and crept samples before and after creep tests was shown in Fig. 15. XRD patterns from the sintered  $\alpha/\beta$ -SiAlON ceramic in Fig. 15 showed large peaks from  $\alpha$ -SiAlON and  $\beta$ -SiAlON, as well as small peaks from other crystalline phase(s).

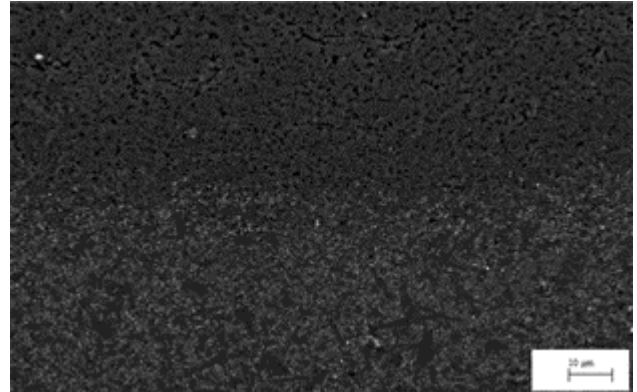


Fig. 12. Back-scattered SEM image of a cross section of the crept specimen (2400 x)

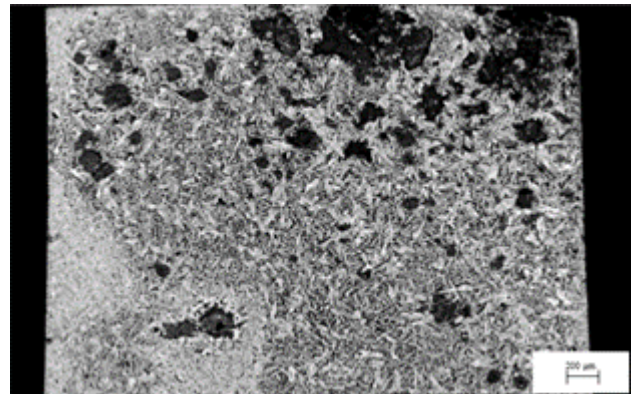


Fig. 13. Back-scattered SEM image of a cross section of the crept specimen (75 x)



Fig. 14. Back-scattered SEM image of a cross section of the crept specimen (1500 x)

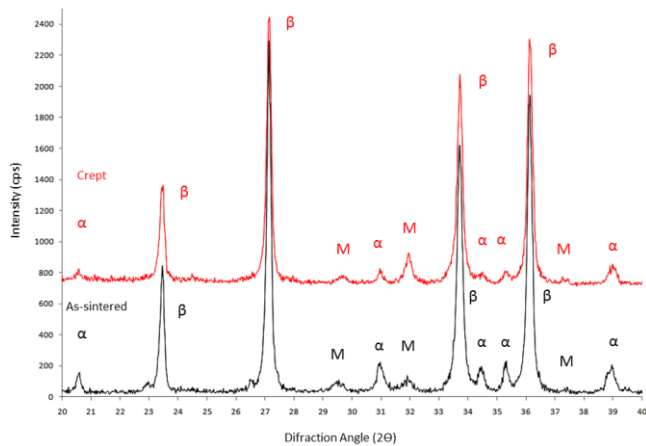


Fig. 15. X-ray diffraction pattern of as-sintered and crept  $\alpha/\beta$ -SiAlON composite ( $\beta$ :beta SiAlON phase,  $\alpha$ :alpha SiAlON phase, M: Melilite phase)

An analysis of the small peaks in the pattern indicated the formation of crystalline aluminum-containing nitrogen melilite phase ( $\text{Ln}_2\text{Si}_{3-x}\text{Al}_x\text{O}_{3+x}\text{N}_{4-x}$ ) (Fig 15). The calculations using the relative intensities from XRD analysis revealed that  $\alpha/\beta$ -SiAlON ratio changed due to the oxidation and the transformation from  $\alpha$ -SiAlON to  $\beta$ -SiAlON. The  $\alpha$ -phase content decreased from 20 to 12% and an increase of intergranular amorphous phase crystallization (as melilite) was observed.

#### IV. CONCLUSIONS

Creep tests are normally performed by applying a constant load/stress and measuring the strain as a function of time. Whereas metallic materials are normally tested in uniaxial tension, the difficulty in producing tensile ceramic specimens, creep data for ceramics are often collected in compression or bending.

In this study four point bending creep tests were conducted in air at temperature of 1400°C and under stress levels ranging from 50 to 150 MPa. Microstructures of SiAlON ceramics were evaluated before and after creep tests.

The formation of melilite phase reduced the creep deformation and this result in the improved creep resistance of these ceramics. Therefore, the SiAlON system presents numerous opportunities for further development. The presence of a number of crystalline secondary phases forming in the system can be utilized for the improvement of high temperature properties.

However, more understanding is needed on the effect of dopant type and composition in order to obtain better crystallization and improved grain boundary chemistry for creep behavior of these ceramics.

#### ACKNOWLEDGMENT

I would like to thank MDA Advanced Ceramic Technology A.S., for supplying of  $\alpha/\beta$ -SiAlON composites, Assistant of Prof. Hilmi Yurdakul and for their help on microscopy investigations and Prof. Dr.

Servet Turan and Associate of Prof. Dilek TURAN for useful discussions..

#### REFERENCES

- [1] Hampshire, S., "Silicon nitride ceramics", Materials Science Forum, 606, 2009, pp. 27-41.
- [2] F.L. Riley, Silicon nitride and related materials, J. Am. Ceram. Soc. 83, (2000), pp. 245-265.
- [3] S. Hampshire, "Silicon nitride ceramics – review of structure, processing and properties", Journal of Achievements in Materials and Manufacturing Engineering, 24, 2007.
- [4] M. H. Bocanegra-Bernal and B. Matovic, "Dense and near-net-shape fabrication of Si<sub>3</sub>N<sub>4</sub> ceramics", Materials Science and Engineering, 5002009, pp.130-149.
- [5] R. F. Coe, R.J. Lumby, M.F. Pawson, Some properties and applications of hot-pressed silicon nitride, in: P. Popper (Ed.), Special Ceramics 5, British Ceramics Association, Stoke-on-Trent, U.K., 1972, pp. 361-376.
- [6] S. Hampshire, M.J. Pomeroy, B. Saruham, in: P. Vincenzini (Ed.), High Tech Ceramics, Elsevier Science Publishers B.V., Amsterdam, 1987, pp. 941-951.
- [7] M.H. Lewis, B.D. Powell, P. Drew, R.J. Lumby, B. North, A.J. Taylor, Formation of single phase Si-Al-O-N ceramics, J. Mater. Sci., 12 (1977), pp. 61.
- [8] G. Ziegler, Thermo-mechanical properties of silicon nitride and their dependence on microstructure, Mater. Sci. Forum 47, (1989), pp. 162-203.
- [9] S. Y. Yoon, S. Y. Kashimura, T. Akatsu, Y. Tanabe, S. Yamada, E. Yasuda, "Grain size dependency on the creep rate in hot-pressed silicon nitride", J. Ceram. Soc. Jpn. 104, (1214), (1996), pp. 939-944.
- [10] S. M. Wiederhorn, A.R. Lopez, W.E. Luecke, M.J. Hoffmann, B.J. Hockey, J.D. French, K.J. Yoon, "Influence of grain size on the tensile creep behavior of ytterbium-containing silicon nitride", J. Am. Ceram. Soc. 87 [3], (2004), pp. 421-30.
- [11] J. A. Schneider, A.K. Mukherjee, "Effects of microstructure on the deformation mechanisms in silicon nitride", J. Am. Ceram. Soc. 82 [3], (1999), pp. 761-764.
- [12] K. M. Fox and J. R. Hellmann, "Microstructure and creep behavior of silicon nitride and SiAlONs", Int. J. Appl. Ceram. Technol. 5, (2008), pp. 138–154.
- [13] S. Hampshire, H. K. Park, D. P. Thompson, K. H. Jack, " $\alpha'$ -Sialon ceramics", Nature 274, (5674), (1978), pp. 880-882.
- [14] T. Ekström, "SiAlON composite ceramics", Key Eng. Mater. 53-55, (1991), pp. 586-591.

[15] T. Ekström, M. Nygren, "SiAlON ceramics", J. Am. Ceram. Soc. 75 (2), (1992), pp. 259-276.

[16] H. Mandal, "New developments in  $\alpha$ -SiAlON ceramics", J. Eur. Ceram. Soc. 19 (13-14), (1999), pp. 2349- 2357.

[17] Lewis, M. H. ve Dobedoe, R. S., "Creep of Ceramics", Encyclopedia of Materials: Science and Technology, 2002.

[18] ENV 820-1, "Advanced technical ceramics - Methods of testing monolithic ceramics -

[19] A. Uludag, D. Turan, "High temperature bending creep behavior of a multi-cation doped  $\alpha$  / $\beta$ -SiAlON composite", Ceramics International 37 (2011) 921–926.